Nanoscale

Cite this: *Nanoscale*, 2011, **3**, 3616

www.rsc.org/nanoscale

COMMUNICATION

Flexible single-walled carbon nanotubes/polyaniline composite films and their enhanced thermoelectric properties†

Jilei Liu, Jing Sun* and Lian Gao

Received 17th April 2011, Accepted 18th July 2011
DOI: 10.1039/c1nr10386e

Flexible single-walled carbon nanotubes/polyaniline (SWNT/PANi) composite films with enhanced thermoelectric properties were prepared *via* a simple method. Furthermore, these paper-like composite films show good flexibility, which makes them possible to be widely applied in various flexible energy converter devices.

Carbon nanotubes/polyaniline (PANi) composites are of tremendous fundamental and technological importance because of their wide applications in electrochemical capacitors,[1–3] disease detection,[4] gas sensing,[5–7] and so on. Recently, the use of CNT/PANi composites as thermoelectric materials has gained interest due to their relatively low thermal conductivity and high electric conductivity, which give them a significant advantage over conventional inorganic thermoelectric materials. Generally, the performance of a thermoelectric material is determined by its dimensionless thermoelectric figure-of-merit, $ZT = \alpha^2\sigma T/\kappa$, where α, σ, T and κ are the Seebeck coefficient, electric conductivity, absolute temperature and thermoelectric conductivity, respectively.[8,9] Multi-walled carbon nanotubes/PANi composites with enhanced thermoelectric properties have been reported by Meng *et al.*[10] More recently, Yao and Chen[11] found that the SWNT/PANi composite prepared by *in situ* chemical polymerization showed enhanced thermoelectric performance, and the maximum power factor of their sample reached 2×10^{-5} W m^{-1} K^{-2}. Therefore, despite relatively little preceding work on the research of thermoelectric performance of CNT/PANi composites until now, their potential application as a kind of novel thermoelectric material has been revealed. To date, the thermoelectric performance of CNT/PANi composites is still too poor to be applied. Therefore, there is a considerable need to learn more details about the effect of microstructure on the thermoelectric performance of CNT/PANi composites. Furthermore, with the development of flexible energy converter devices, the exploration of preparing flexible thermoelectric materials in a simple way is meaningful and challengeable.

In this communication, attempts have been made for the preparation of flexible SWNT/PANi composite films with enhanced thermoelectric properties. The *in situ* electrochemical polymerization process was employed because it can sensitively adjust the morphology and microstructure of the PANi composites through subtle modulation of the electrolyte component and electric current,[12,13] which make it convenient to give more insight about the effect of microstructure on their thermoelectric performance.

Electrochemical deposition of paper-like SWNT/PANi composite films was carried out in a three-electrode cell (see Fig. 1), where SWNT buckypaper, platinum wire and SCE were used as the working electrode, the counter electrode and the reference electrode, respectively. By controlling the electrodeposited cycles at 25, 50, 75, and 100, we obtained the composite films SWNT/PANi25, SWNT/PANi50, SWNT/PANi75, and SWNT/PANi100, respectively. For comparison, pure PANi films were grown on a titanium plate under the same conditions.

Fig. 2 presents the field emission scanning electron microscopy (FE-SEM) and transmission electron microscopy (TEM) images of SWNT/PANi composite films with different electrodeposited cycles. As was typical for SWNT networks, the resultant SWNT/PANi composite bundles randomly interwound together to form three-dimensional (3D) networks with wide bundle diameter distribution. An increase in the diameter of SWNT/PANi composites is observed from Fig. 2a–e, which indicates that more and more PANi was electrodeposited onto the surface of SWNT sheets with prolongation

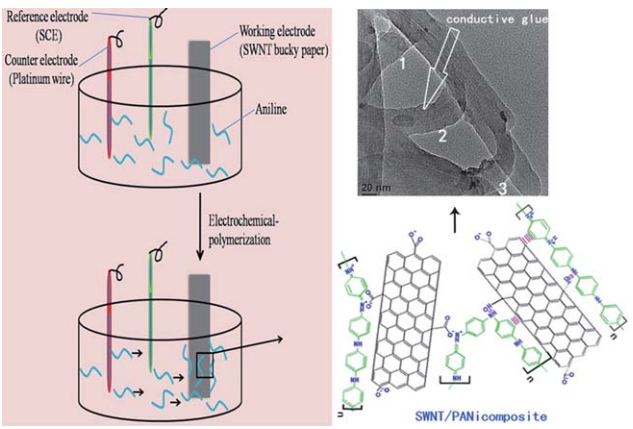

Fig. 1 Schematic diagram illustrating the formation process of flexible SWNT/PANi composite films during electrodeposition of PANi onto the surface of the working electrode, and their possible formation mechanism involved in the interaction between PANi and acid-treated SWNTs. The inset shows a TEM image of the "conductive glue".

State Key Lab of High Performance Ceramics and Superfine Microstructure, Shanghai Institute of Ceramic, Chinese Academy of Sciences, Shanghai, 200050, China. E-mail: jingsun@mail.sic.ac.cn

† Electronic supplementary information (ESI) available. See DOI: 10.1039/c1nr10386e

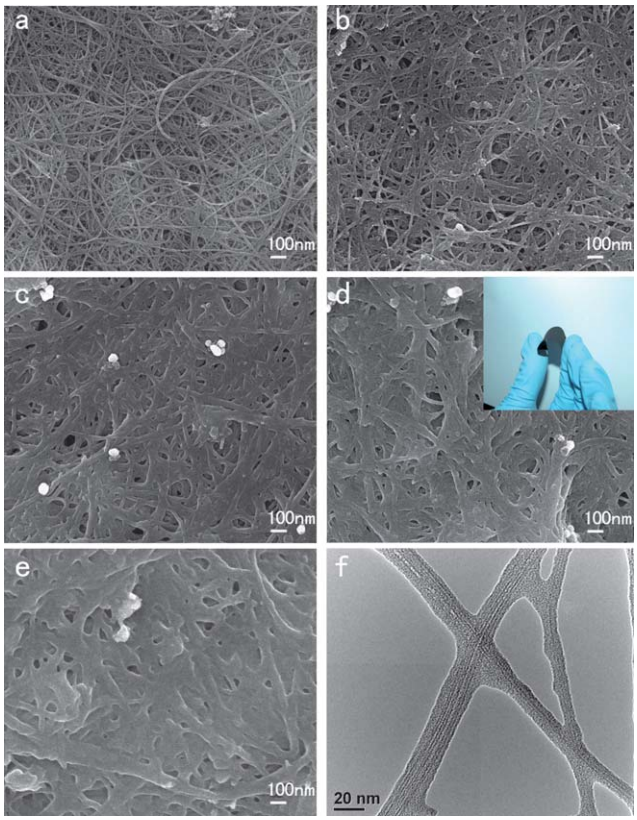

Fig. 2 Scanning electron microscopy (SEM) images of (a) pure SWNT paper, as well as SWNT/PANi composite films (b) SWNT/PANi25, (c) SWNT/PANi50, (d) SWNT/PANi75 and (e) SWNT/PANi100, at the same magnification. The inset in panel (d) is a digital macrograph of the flexible composite film. (f) TEM image of SWNT/PANi50.

of the electro-polymerization process. The inset in Fig. 2d shows the good flexibility of paper-like SWNT/PANi composite films. They can be rolled up, bent, and even twisted without cracking, this unique mechanical property is superior to that of the conventional inorganic thermoelectric material and makes them possible to be applied in flexible energy converter systems. The typical tubular-shell nanostructure of individual SWNT and SWNT bundles coated with PANi is demonstrated in the TEM image in Fig. 2f.

Raman spectroscopy was also used to characterize the change in microstructure of different SWNT/PANi composite films. As shown in Fig. 3, Raman spectra of SWNT/PANi composite films are similar to that of pure PANi, revealing that acid-treated SWNTs serve as the core in the formation of the tubular shell SWNT/PANi composites.[14] Note that the intensity of Raman peaks at 1160 and 1485 cm^{-1}, which correspond to C–H bending of the quinoid ring and C═N stretching of the quinoid ring, respectively,[15,16] increases as the number of electro-polymerization cycles increases, indicating that more and more PANi was electrodeposited onto the paper-like SWNT films.

Fig. 4 and Table 1 compare the room temperature Seebeck coefficient, the electric conductivity and the corresponding power factor of SWNT/PANi composite films as a function of electro-polymerization cycles. In the present experiments, the pure SWNT buckypaper shows excellent electrical conductivity, about 3373 S m^{-1} was obtained. While the value decreased for SWNT/PANi composite films owing to the poor electric conductivity of PANi as well as their block or scatter effect of carriers.[10] Measured carrier density and

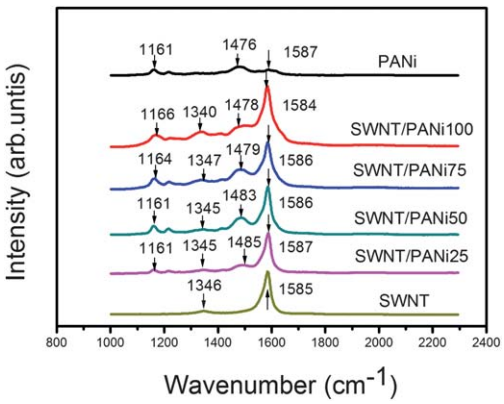

Fig. 3 Raman spectra ($\lambda_{exp} = 532$ nm) of pure SWNT paper, pure PANi, and SWNT/PANi composite films with different electrochemical polymerization cycles (25, 50, 75 and 100, respectively).

carrier mobilities are given in Table 2, in order to support our conclusion. It was noticed that the carrier mobility changed in the same way as that of electric conductivity, which indicates that changes in electric conductivity mainly came from carrier mobility. The variation in carrier mobility as well as electric conductivity could be explained explicitly from the formation mechanism of tubular SWNT/PANi composites. In the initial stage of the electro-polymerization process, the π-bonded surface of the SWNTs interacted strongly with the conjugated structure of PANi, which facilitated the deposition of polymer chains onto the surface of PANi, forming a tubular coated layer (shown in Fig. 2f). Here, the SWNT network served as the core and self-assembly template for accelerating the nucleation and the growth of PANi. On one hand, the electric conductivity of the PANi coated layer itself is very poor (as shown in Table 2, the carrier mobility of pure PANi films is only 0.39, which is far less than that of pure SWNT films); on the other hand, the PANi coated layer could scatter or block transport of carriers along the CNT chains, both of them resulted in the decrease in carrier mobility and electric conductivity of SWNT/PANi composite films from pure SWNT to SWNT/PANi50. Meanwhile, an increase in carrier density was noticed, which was attributed to the enhancement in quantum-confinement effects of the charge carriers and the strong interaction between flat PANi and SWNTs, where positive charges induced on the polymer chains were compensated by the anion-charged carboxyl-group-functionalized composites, as shown in Fig. 1 (SWNT/PANi composites). A charge-transfer reaction related to the

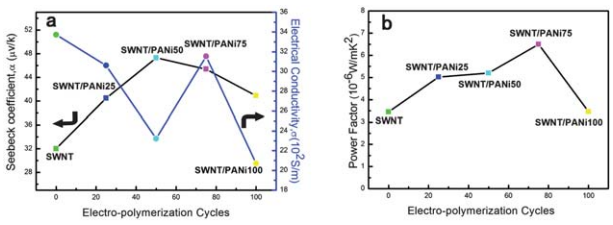

Fig. 4 (a) The Seebeck coefficient (filled squares) and electric conductivity (filled circles), (b) power factor of pure SWNT paper and SWNT/PANi composite films with electrochemical polymerization cycles at 25, 50, 75, and 100 respectively. (The arrows in panel (a) point to different *y*-axis labels.)

Table 1 The Seebeck coefficient, electric conductivity and power factor of resulting SWNT/PANi composite films

Sample	Seebeck coefficient/ $\mu V\ K^{-1}$	Electric conductivity/ $10^2\ S\ m^{-1}$	Power factor/ $\mu W\ m^{-1}\ K^{-2}$
Pure SWNT	32	33.73	3.45
SWNT/PANi25	40.5	30.6	5.02
SWNT/PANi50	47.3	23.23	5.20
SWNT/PANi75	45.4	31.53	6.50
SWNT/PANi100	40.9	20.7	3.46
Pure PANi	10.1	0.97	0.0098

strong interaction between PANi and SWNT occurred, which is similar to a doping process, modulating the Fermi level of SWNTs and thus giving rise to the increase in carrier density. Interestingly, an increase in electric conductivity from sample SWNT/PANi50 to SWNT/PANi75 was observed. The replacement of the junction forms of SWNT/SWNT with SWNT/PANi/SWNT in composite films is responsible for the improvement of electrical conductivity. PANi acts as "conductive glue", effectively assembling the SWNTs into a conductive network, which facilitated the transfer of charge carriers, and thus increase the electric conductivity. As shown in Fig. 1 (TEM image), SWNT (core) well coated with PANi (shell) interwound with each other to form a homogeneous conductive network, where PANi works as "conductive glue" to bring SWNT together and promote the transfer of charge carrier between SWNT and PANi (an increase in the carrier mobility from SWNT/PANi50 to SWNT/PANi75 is noticed in Table 2). More importantly, as the polymerization continues, thicker PANi layers formed on the surface of SWNTs, causing weaker interaction between PANi and SWNTs. Thus, some disordered PANi formed at off-laying spaces that surrounded the ordered polycrystalline regions (which are confirmed in Fig. S1†) and resulted in weaker scatter effects, thus increase the carrier mobility. However, as the electrochemical polymerization process continued, more and more disordered PANi were deposited, their poor electric conductivity (usually, the electric conductivity of disordered PANi is inferior to that of polycrystalline PANi) resulted in the slight decrease in carrier mobility for SWNT/PANi100. Our explanation above was further verified by the decrease in carrier density from sample SWNT/PANi75 to SWNT/PANi100, which was attributed to the weaker quantum-confinement effects and weaker interaction between PANi and SWNTs related to the increase in the thickness of the PANi coated layer.

Seebeck coefficients of different samples are also shown in Fig. 4a. It is clear that the Seebeck coefficient showed an inverse tendency compared to that of electric conductivity, which is in agreement with earlier studies of conductive polymers.[9,17] The Seebeck coefficient

Table 2 Electric conductivity, carrier mobility and carrier density of resulting SWNT/PANi composite films

Sample	Electric conductivity/ $10^2\ S\ m^{-1}$	Carrier density/ $10^{20}\ cm^{-3}$	Carrier mobility / $cm^2\ V^{-1}\ s^{-1}$
Pure SWNT	33.73	0.73	2.88
SWNT/PANi25	30.6	0.86	2.22
SWNT/PANi50	23.23	2.20	0.66
SWNT/PANi75	31.53	1.25	1.57
SWNT/PANi100	20.7	0.95	1.36
Pure PANi	0.97	0.16	0.39

increased with the increase of electro-polymerization cycles, when the number of electro-polymerization cycles reached 50, the maximum Seebeck coefficient, 47.3 $\mu V\ K^{-1}$, was obtained, and then decreased with further increasing electrodeposited cycles. A value of 40.9 $\mu V\ K^{-1}$ was obtained for sample SWNT/PANi100, which is nearly 14% less than that of SWNT/PANi50. Similar to the analysis of electric conductivity mentioned above, the variation in the Seebeck coefficient originates from the change in doping in SWNTs and how charges are transferred in SWNT/PANi composite films with the increase in polymerization cycles, therefore, it can also be explained from the formation process of SWNT/PANi composites. In the initial stage of the *in situ* electrochemical polymerization process, PANi mainly exists in the polycrystalline form due to the strong interaction between the π-bonded surface of the SWNTs and the conjugated structure of PANi.[3] The surrounding polycrystalline PANi coated layer results in the enhancement in electron energy filtering effects of SWNT/PANi composite films by blocking or scattering the transport of some carriers along the carbon nanotubes chain, which is similar to the screening of electrons by potential wells in inorganic materials, thus enhancing the Seebeck coefficient and reducing the electric conductivity.[10,17–19] However, when more and more PANi were electrodeposited, for this kind of unique 1-dimensional SWNT (tubular)–PANi (shell) nanostructure, the increase in thickness of the PANi coated layer on one hand would result in a decrease in size-dependent energy filtering effect[10,20] and on the other hand would give rise to the formation of disordered PANi due to the weak interaction between the polymer and charged SWNTs (which are verified by Fig. S1†, where the selected area electron diffraction patterns show more and more amorphous rings with the increase of electro-polymerization cycles), both of which result in a decrease of the Seebeck coefficient.

The power factor ($\alpha^2\sigma$) was calculated based on the values of Seebeck coefficient and electric conductivity (shown in Fig. 4b). The maximum power factor, 6.5×10^{-6}, was obtained for sample SWNT/PANi75, which was almost two times that of pure SWNT buckypaper. Note that from pure SWNT sheet to SWNT/PANi75, the power factor increases gradually, which suggests that although the Seebeck coefficient and electric conductivity take on a nearly inverse trend, the reduction in the electric conductivity is more than compensated by the increase in the Seebeck coefficient,[21] thereby resulting in an increase in power factor. This unique relationship between the Seebeck coefficient and electric conductivity makes it possible to strike a balance in the composition of SWNT/PANi composite films such that the relatively high Seebeck coefficient and electric conductivity can be obtained simultaneously to obtain a maximum power factor. A promising approach is to give more control on the microstructure of SWNT/PANi composite films, such as controlling the thickness of the PANi coated layer, modulating the orientation of plain PANi along the axis of SWNT, removing the off-laying disordered PANi, *etc.* Our later work is focusing on these.

Conclusions

In summary, flexible SWNT/PANi composite films with enhanced thermoelectric performance were prepared *via* a simple method, and their thermoelectric properties—Seebeck coefficient, electric conductivity and power factor—were measured as a function of electrochemical polymerization cycles. The enhanced Seebeck coefficient and power factor were obtained, which were attributed to the change

in the doping in SWNTs and size-dependent electron energy filtering effects related to the unique SWNT (tubular)–PANi (shell) tubular nanostructure. Furthermore, they show good flexibility, which make them possible to be applied in various flexible energy devices.

Acknowledgements

This work is supported by the National Science Foundation of China (no. 50972153, 50972157, 51072215) and Shanghai Committee of Science and Technology (no. 10DZ0505000).

Notes and references

1 S. R. Sivakkumar, W. J. Kim and M. Forsyth, *J. Power Sources*, 2007, **171**, 1062–1068.
2 E. Frackowiak, V. Khomenko, K. Jurewicz, K. Lota and F. Beguin, *J. Power Sources*, 2006, **153**, 413–418.
3 X. F. Xie, L. Gao, J. Sun and Y. Q. Liu, *Carbon*, 2008, **46**, 1145–1151.
4 R. Singh and C. Dhand, *J. Mol. Recognit.*, 2010, **23**, 472–479.
5 C. Dhand and P. R. Solanki, *Electroanalysis*, 2010, **22**, 2683–2693.
6 R. E. Sabzi and K. Rezapour, *J. Serb. Chem. Soc.*, 2010, **75**, 537–549.
7 M. G. Ding, Y. F. Tang, P. P. Gou, M. J. Reber and A. Star, *Adv. Mater.*, 2011, **23**, 536–540.
8 H. J. Goldsmid, *Thermoelectric Refrigeration*, Plenum, New York, 1964.
9 I. Levesque and P. O. Bertrand, *Chem. Mater.*, 2007, **19**, 2128–2138.
10 C. Z. Meng, C. H. Liu and S. S. Fan, *Adv. Mater.*, 2010, **22**, 535–539.
11 Q. Yao and L. D. Chen, *ACS Nano*, 2010, **4**, 2445–2451.
12 C. C. Hu and C. H. Chu, *Mater. Chem. Phys.*, 2000, **65**, 329–338.
13 Z. Wang, J. Yuan and M. Li, *J. Electroanal. Chem.*, 2007, **599**, 121–126.
14 T. M. Wu and Y. W. Lin, *Polymer*, 2006, **47**, 3576–3582.
15 M. Cochet, G. Louarn, S. Quillard, J. P. Buisson and S. Lefrant, *J. Raman Spectrosc.*, 2000, **31**, 1041–1049.
16 S. Quillard, G. Louarn and S. Lefrant, *Phys. Rev. B: Condens. Matter*, 1994, **50**, 12496–12508.
17 K. C. Chang, M. S. Jeng, C. C. Yang, Y. W. Chou, S. K. Wu, M. A. Thomas and Y. C. Peng, *J. Electron. Mater.*, 2009, **38**, 1182–1188.
18 G. D. Zhan, J. D. Kuntz, A. K. Mukherjee, P. Zhu and K. Koumoto, *Scr. Mater.*, 2006, **54**, 77–82.
19 M. S. Dresselhaus, G. Chen, M. Y. Tang, R. G. Yang, H. Lee and P. Gogna, *Adv. Mater.*, 2007, **19**, 1043–1053.
20 L. D. Hicks and M. S. Dresselhaus, *Phys. Rev. B: Condens. Matter*, 1993, **47**, 12727–12731.
21 J. P. Heremans and C. M. Jaworski, *Appl. Phys. Lett.*, 2008, **93**, 122107.